



Advanced optical magnetic nanostructures fabricated by anodic aluminum oxide membranes and magnetic fluids

Ziyun Di, Xianfeng Chen, and Dongchen Zhang

Citation: *J. Appl. Phys.* **106**, 073101 (2009); doi: 10.1063/1.3226861

View online: <http://dx.doi.org/10.1063/1.3226861>

View Table of Contents: <http://jap.aip.org/resource/1/JAPIAU/v106/i7>

Published by the **AIP Publishing LLC**.

Additional information on *J. Appl. Phys.*

Journal Homepage: <http://jap.aip.org/>

Journal Information: http://jap.aip.org/about/about_the_journal

Top downloads: http://jap.aip.org/features/most_downloaded

Information for Authors: <http://jap.aip.org/authors>

ADVERTISEMENT



**Running in Circles Looking
for the Best Science Job?**

Search hundreds of exciting
new jobs each month!

<http://careers.physicstoday.org/jobs>

physicstodayJOBS



Advanced optical magnetic nanostructures fabricated by anodic aluminum oxide membranes and magnetic fluids

Ziyun Di, Xianfeng Chen,^{a)} and Dongchen Zhang

Department of Physics, State Key Laboratory on Fiber Optic Local Area Communication Networks and Advanced Optical Communication Systems, Shanghai Jiao Tong University, Shanghai 200240, China

(Received 23 July 2009; accepted 21 August 2009; published online 2 October 2009)

Optical magnetic nanostructures, based on anodic aluminum oxide membranes and magnetic fluids, were fabricated and investigated in both transmission and magneto-optical properties. A strong enhancement in transmission property has been found compared with the traditional magnetic fluids. Excellent magneto-optical characteristic was obtained: a negative differential magnetic linear dichroism was observed, quite different from the traditional Langevin type of magnetic fluids. This phenomenon was interpreted by an antiferromagnetic coupling between two types of magnetic grains having different average diameters in the nanocomposites. Based on its outstanding magneto-optical effects, it may open potentials for future integral optical devices. © 2009 American Institute of Physics. [doi:10.1063/1.3226861]

I. INTRODUCTION

There has been a strong effect to probe optical magnetic nanostructures because of their potential applications in magneto-optical switches, modulators, optical circulators, laser isolators, magnetic field, and electric current sensors based on their multiple magneto-optical effects.^{1–5} The entrapment of magnetic nanoparticles into solid matrices is nowadays attracting much more interest. Most of these works were devoted to studying magnetic nanoparticles dispersed in polymer matrices, in silica gels, or grown into porous colloidal silica particles.^{6–9} However, a meaningful challenge lies in simultaneously achieving “transparent” optical properties (because of the high absorption coefficients of the magnetic particles) with excellent magneto-optical effects, and reducing the size of the magnetic particles in the composite in order to obtain superparamagnetic behavior making the sample to be sensible at low magnetic fields.

Porous alumina films formed by anodic oxidation of aluminum have been intensively studied for use as molds to form nanostructured materials. There is a great demand for the use of highly ordered nanohole arrays in a diversity of applications, such as high-density storage media, functional nanomaterials exhibiting quantum size effect, nanoelectronic devices, and functional biochemical membranes.^{10–14} Magnetic materials embedded in porous alumina matrix have a long history.^{15–17} Generally, the main purpose of these studies is to realize a high-density magnetic recording media.^{18–20} However, the idea of using nanoporous anodized aluminum oxide (AAO) membranes embedded with magnetic nanoparticles for optical application has not yet been much reported. This technique is promising for meeting the challenge mentioned above since it is compatible with both nanofabrication and magneto-optical studies.

In this paper, we have demonstrated a brand new method to obtain AAO/Fe₃O₄ magnetic nanocomposites from AAO

membrane in magnetic fluids (MFs). [MF is a stable colloid consisting of finely divided single-domain magnetic nanoparticles (usually 3–15 nm in diameter) coated with a molecular layer of dispersant and dispersed in a suitable liquid carrier.]^{21–24} The optical and magneto-optical properties of Fe₃O₄ nanoparticles with an average size of 10 nm, embedded in nanoporous AAO membranes, were studied. The (AAO/Fe₃O₄)₇₀ (pore diameter $d=70$ nm) nanocomposite showed not only good optical transmission property, but also remarkable magnetic linear dichroism (MLD) effect. The negative differential MLD phenomenon was interpreted by an antiferromagnetic coupling between two types of magnetic grains having different average diameters in the (AAO/Fe₃O₄)₇₀ nanocomposites.

II. EXPERIMENTAL

Figure 1(a) is a schematic picture of the commercial nanoporous AAO membrane with the nanohole array open in both upper and bottom sides. A plan view field emission scanning electron microscopy (FE-SEM) image [Fig. 1(b)] shows a hexagonal close-packed arrays of nanoholes with an average diameter of 50 nm. The distance between these nanohole arrays is 100 nm, and the neighboring nanoholes are separated by a 50-nm-thick Al₂O₃ sidewall. The depth of each nanohole array equals to the height of the membrane 40 μm. Figure 1(c) is the cross-sectional view FE-SEM image of the AAO membrane. Figures 1(b) and 1(c) show a high quality AAO membrane. The commercial MF we used here was a water-based Fe₃O₄ MF with an average particle diameter of 10 nm. Here we used a chemical-free way to form the AAO/Fe₃O₄ nanocomposite at room temperature. The AAO membrane was immersed in a 3% water-based Fe₃O₄ MF with an average particle diameter of 10 nm. The MF together with the AAO membrane was put in an airtight environment. All we used here was to vacuumize to let the solution infiltrated into the holes of the AAO membrane. The solution-filled AAO membrane was precleaned in water for

^{a)}Electronic mail: xfchen@sjtu.edu.cn.

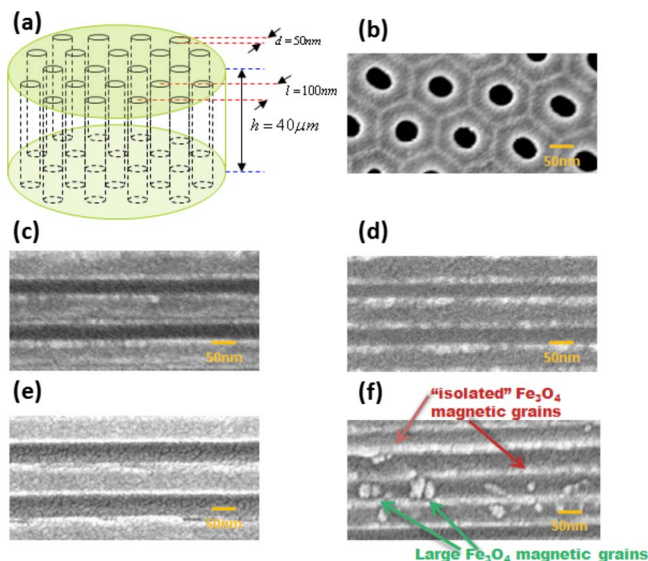


FIG. 1. (Color online) (a) A schematic picture of the commercial nanoporous AAO membrane with the nanohole array open in both upper and bottom sides. (b) A top view FE-SEM image of AAO membrane with the pore diameter d of 50 nm. (c) The cross-sectional view FE-SEM image of the AAO membrane ($d=50$ nm). (d) The cross-sectional view FE-SEM image of AAO membrane ($d=50$ nm) filled with the Fe_3O_4 nanoparticles: $(\text{AAO}/\text{Fe}_3\text{O}_4)_{50}$. (e) The cross-sectional view FE-SEM image of the AAO membrane ($d=70$ nm). (f) The cross-sectional view FE-SEM image of AAO membrane ($d=70$ nm) filled with the Fe_3O_4 nanoparticles: $(\text{AAO}/\text{Fe}_3\text{O}_4)_{70}$.

several seconds and then air-dried for 2 h. After that, a thin porous AAO membrane filled with 10 nm Fe_3O_4 particles was formed.

The FE-SEM pictures have been taken on samples $[(\text{AAO}/\text{Fe}_3\text{O}_4)_{50}, (\text{AAO}/\text{Fe}_3\text{O}_4)_{70}]$ with the pore diameter d of 50 and 70 nm, respectively. The cross section picture taken on $(\text{AAO}/\text{Fe}_3\text{O}_4)_{50}$ [Fig. 1(d)] shows no obvious large Fe_3O_4 grains inside or on the inner sidewall of nanohole arrays. And we obtained the same results in the different areas of different $(\text{AAO}/\text{Fe}_3\text{O}_4)_{50}$ samples under the same procedures. However, we were excited to find some obvious “isolated” Fe_3O_4 magnetic grains and some large Fe_3O_4 magnetic grains inside nanohole arrays sandwiched between Al_2O_3 sidewalls in the $(\text{AAO}/\text{Fe}_3\text{O}_4)_{70}$ case [Fig. 1(f)]. Comparing Fig. 1(d) with Fig. 1(f), one can see that increasing the pore diameter d of the AAO membrane proved effective for Fe_3O_4 nanoparticles to transfer into the nanohole arrays. The reason for having two different magnetic size scales for the Fe_3O_4 grains has not been clarified yet. Actually, we can imagine that, besides a large number of isolated particles, there are a lot of dense ferrocoupled domains on the inner sidewall of nanoholes.

III. RESULTS AND DISCUSSION

Figure 2 is an absorption spectrum of the nanocomposite $(\text{AAO}/\text{Fe}_3\text{O}_4)_{70}$ and the MF with the same thickness. Here we only listed the absorption spectrum of the nanocomposite $(\text{AAO}/\text{Fe}_3\text{O}_4)_{70}$, not the nanocomposite $(\text{AAO}/\text{Fe}_3\text{O}_4)_{50}$ because apparently, from the FE-SEM image showed in Fig. 1(d), the nanocomposite $(\text{AAO}/\text{Fe}_3\text{O}_4)_{50}$ did not turn out well, which will also be testified in Figs. 3 and 4. By using

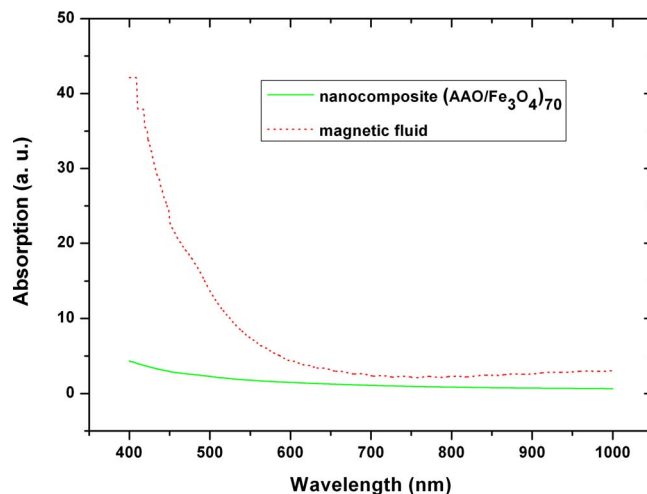


FIG. 2. (Color online) Absorption spectrum of the nanocomposite $(\text{AAO}/\text{Fe}_3\text{O}_4)_{70}$ and MF with the same thickness of 40 μm .

the equation of $\alpha = -\ln T$ (here α is the absorption and T is the transmittance) we can find out that $T=23\%$ for $(\text{AAO}/\text{Fe}_3\text{O}_4)_{70}$, and $T=1\%$ for MF at the wavelength of 600 nm. It is seen from Fig. 2 that there is a large improvement in the light transmission property compared with the traditional MF with the same thickness (Fig. 2) and the composites consisting of magnetic nanoparticles dispersed in polymer matrices.^{6,25}

The transmitted light (wavelength 632.8 nm) intensity with the electric vector perpendicular ($\theta=90^\circ$) and parallel ($\theta=0^\circ$) to the magnetic field, respectively, for nanocomposite $(\text{AAO}/\text{Fe}_3\text{O}_4)_{50}$ and $(\text{AAO}/\text{Fe}_3\text{O}_4)_{70}$ versus magnetic field at room temperature was measured (shown in Fig. 3). Their behaviors were different for different nanocomposites. As for the nanocomposite $(\text{AAO}/\text{Fe}_3\text{O}_4)_{50}$ case, the normalized transmitted light intensity remained almost still with the increasing field strength, which meant that the magnetic Fe_3O_4 nanoparticle did not play an important role in the light transmission under the field. Interestingly, as for the

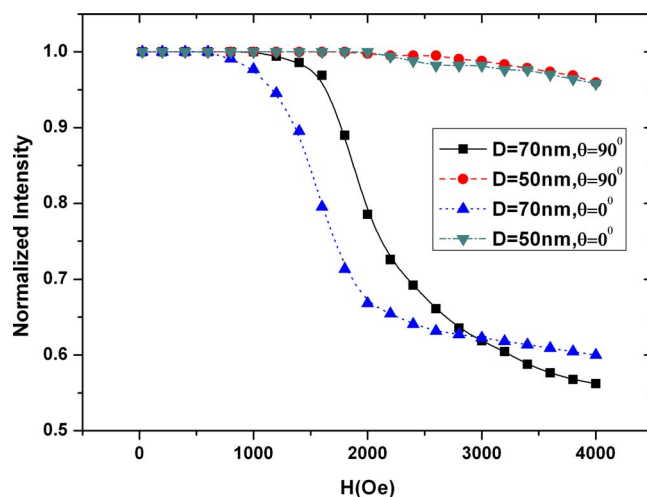


FIG. 3. (Color online) The normalized transmitted light intensity with the electric vector perpendicular ($\theta=90^\circ$) and parallel ($\theta=0^\circ$) to the magnetic field, respectively, for nanocomposite $(\text{AAO}/\text{Fe}_3\text{O}_4)_{50}$ (pore diameter $d=50$ nm) and $(\text{AAO}/\text{Fe}_3\text{O}_4)_{70}$ (pore diameter $d=70$ nm) vs magnetic fields.

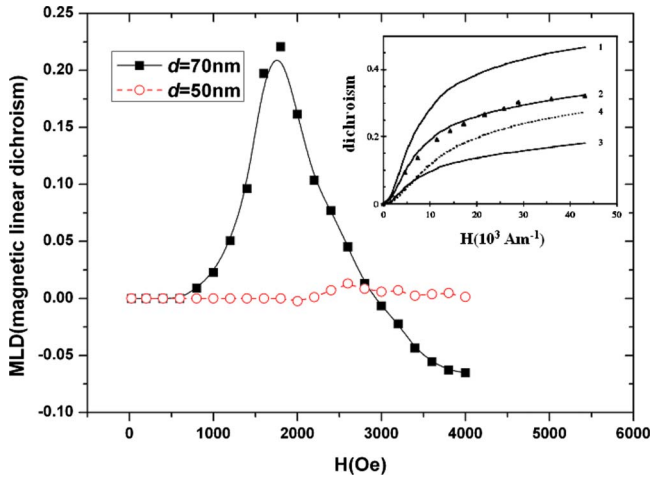


FIG. 4. (Color online) The MLD of the nanocomposites $(\text{AAO}/\text{Fe}_3\text{O}_4)_{50}$ (pore diameter $d=50$ nm) and $(\text{AAO}/\text{Fe}_3\text{O}_4)_{70}$ (pore diameter $d=70$ nm) as a function of magnetic field. The inset shows the MLD picture of the traditional Langevin type of MFs (Ref. 28).

$(\text{AAO}/\text{Fe}_3\text{O}_4)_{70}$, the light transmission of both the $\theta=90^\circ$ and $\theta=0^\circ$ cases showed a monotonic decreasing with H while in the larger field region tending to saturated, but the beginning point where it started to decrease was different.

The MLD of the nanocomposites $[(\text{AAO}/\text{Fe}_3\text{O}_4)_{50}$ and $(\text{AAO}/\text{Fe}_3\text{O}_4)_{70}]$ as a function of magnetic field strength is shown in Fig. 4. The values of the parallel and perpendicular dichroism $\Delta\alpha_{\parallel}$ and $\Delta\alpha_{\perp}$, are defined as the change in the absorbance of the sample as a result of applying a magnetic field and are given by

$$\Delta\alpha_{\parallel} = -\ln(I_{\parallel}/I_0),$$

$$\Delta\alpha_{\perp} = -\ln(I_{\perp}/I_0),$$

where I_0 is the transmitted intensity at zero field. The MLD $\Delta\alpha$ is then given by

$$\Delta\alpha = \Delta\alpha_{\parallel} - \Delta\alpha_{\perp}.$$

According to Fig. 4, the MLD signals of the composite $(\text{AAO}/\text{Fe}_3\text{O}_4)_{50}$ equal almost to zero, which indicates that the wish of putting Fe_3O_4 nanoparticles into the nanoholes fails, consistent with the results we got in Fig. 1(d) and Fig. 3. However, the situation of the MLD signals differs greatly for the composite $(\text{AAO}/\text{Fe}_3\text{O}_4)_{70}$. The MLD signals experienced a continuous enhancement up to the field strength of 1800 Oe, and dropped greatly with the increasing field strength. Surprisingly, a negative differential MLD was observed at the field strength of 1800 Oe, quite different from the traditional Langevin type,^{26–28} which also declares the success of the optical magnetic nanocomposite $(\text{AAO}/\text{Fe}_3\text{O}_4)_{70}$.

Actually, the usual peak in Fig. 4 indicates the existence of antiferromagnetic coupling and antiferromagnetic exchange interactions in the nanocomposites $(\text{AAO}/\text{Fe}_3\text{O}_4)_{70}$. Magnetic nanosized materials display a variety of unusual hysteresis loops, for the explanation of which several different models and possible physical mechanisms have been proposed.^{29–33} Here, we discuss briefly the possible origin of the anomalous behavior compared with the conventional MF.

There are two types of magnetic Fe_3O_4 grains: the isolated magnetic grains and the large Fe_3O_4 magnetic grains [Fig. 1(f)], and we mark them as “I” and “II” grains, respectively. In real materials, the system always finds the configuration of absolute minimum energy. The internal energy of the system is given by³⁴

$$E = a \cos(\theta_1 - \theta_2) - b(\cos \theta_1 + \cos \theta_2) + E_{A1} + E_{A2},$$

where a is the coupling strength between the nanodomains, b is the applied magnetic field, θ_1 and θ_2 are the angular positions of the moments with respect to the applied field, and E_{A1} and E_{A2} represent the in-plane anisotropy energy. Based on this model the coupling is allowed to be ferromagnetic ($a < 0$) or antiferromagnetic ($a > 0$). Initially, in the low field range, the thermal activation plays the most important role on the magnetic state of the system, so the magnetization is just the weighted average of the two Langevin functions of I and II grains. After that, let us assume that fields higher than 1800 Oe are large enough to make the antiferromagnetic coupling between some of the I and II grains happen, and their magnetic moments are antiparallel, eventually leading to the decrease in the total magnetization. Further increase in the field can make the moment of I and II grains orientate again through the spin-flopping, characteristic for antiferromagnets. We believe that the roughness of the Al_2O_3 sidewall might be one of the reasons why there are two types of magnetic grains in the composites and this antiferromagnetic coupling might happen both in the intralayer and interlayer of the nanocomposites. Meanwhile, according to Ref. 35, there is also a possibility that magnetostatic effects would lead to ferromagnetic order or antiferromagnetic order depending on whether the field is applied along or perpendicular to the direction of particle interaction.

IV. CONCLUSIONS

In summary, we have designed and fabricated the optical magnetic nanostructures using AAO membranes and MFs $[(\text{AAO}/\text{Fe}_3\text{O}_4)_{50}, (\text{AAO}/\text{Fe}_3\text{O}_4)_{70}]$. The $\text{AAO}/\text{Fe}_3\text{O}_4$ nanocomposites were studied by optical transmission and magneto-optical effects. It turned out that the pore diameter $d=50$ nm AAO membranes were not appropriate for $\text{AAO}/\text{Fe}_3\text{O}_4$ nanocomposite, according to the FE-SEM image and the magneto-optical investigation. The $(\text{AAO}/\text{Fe}_3\text{O}_4)_{70}$ (pore diameter $d=70$ nm) case showed a high quality of absorption spectrum and an unusual peak in the field dependent MLD. This phenomenon was interpreted by an antiferromagnetic coupling between two types of magnetic grains having different average diameters in the composites.

ACKNOWLEDGMENTS

This research was supported by the National Natural Science Foundation of China (Grant No. 10874119); the National Basic Research Program “973” of China (Grant No. 2007CB307000); and the Shanghai Leading Academic Discipline Project (Grant No. B201); and Instrumental Analysis Center, Shanghai Jiao Tong University.

- ¹N. Qureshi, H. Schmidt, and A. R. Hawkins, *Appl. Phys. Lett.* **85**, 431 (2004).
- ²V. Pavlov, P. Usachev, R. Pisarev, D. Kurdyukov, S. Kaplan, A. Kimel, A. Kirilyuk, and Th. Rasing, *Appl. Phys. Lett.* **93**, 072502 (2008).
- ³R. J. Martín-Palma, M. Manso, M. Arroyo-Hernández, V. Torres-Costa, and J. M. Martínez-Duart, *Appl. Phys. Lett.* **89**, 053126 (2006).
- ⁴E. Céspedes, Y. Huttel, L. Martínez, A. de Andrés, J. Chaboy, M. Vila, N. D. Telling, G. van der Laan, and C. Prieto, *Appl. Phys. Lett.* **93**, 252506 (2008).
- ⁵H. Liu, J. Wu, J. Min, and Y. Kim, *J. Appl. Phys.* **103**, 07D529 (2008).
- ⁶C. R. Mayer, V. Cabuil, T. Lalot, and R. Thouvenot, *Adv. Mater.* **12**, 417 (2000).
- ⁷C. Chanéac, E. Tronc, and J. P. Jolivet, *J. Mater. Chem.* **6**, 1905 (1996).
- ⁸S. Sonlinas, G. Piccaluga, M. P. Morales, and C. J. Sema, *Acta Mater.* **49**, 2805 (2001).
- ⁹P. Tartaj, T. González-Carreño, and C. Serna, *Adv. Mater.* **13**, 1620 (2001).
- ¹⁰S. Kim, J. Lee, Y. Chang, S. Hwang, and K.-H. Yoo, *Appl. Phys. Lett.* **93**, 033503 (2008).
- ¹¹M. Tofizur Rahman, R. K. Dumas, N. Eibagi, N. N. Shams, Y.-C. Wu, K. Liu, and C.-H. Lai, *Appl. Phys. Lett.* **94**, 042507 (2009).
- ¹²J. Gao, Q. Zhan, W. He, D. Sun, and Z. Cheng, *Appl. Phys. Lett.* **86**, 232506 (2005).
- ¹³K. Y. Zang, S. J. Chua, J. H. Teng, N. S. S. Ang, A. M. Yong, and S. Y. Chow, *Appl. Phys. Lett.* **92**, 243126 (2008).
- ¹⁴E. A. Bluhm, E. Bauer, R. M. Chamberlin, K. D. Abney, J. S. Young, and G. D. Jarvinen, *Langmuir* **15**, 8668 (1999).
- ¹⁵S. Kawai and I. Ishiguro, *J. Electrochem. Soc.* **122**, 32 (1975).
- ¹⁶G. J. Strijkers, J. H. J. Dalderop, M. A. A. Broeksteeg, H. J. M. Swagten, and W. J. M. de Jonge, *J. Appl. Phys.* **86**, 5141 (1999).
- ¹⁷K. Nielsch, F. Muller, A. P. Li, and U. Gosele, *Adv. Mater.* **12**, 582 (2000).
- ¹⁸S. Sun, D. Weller, and C. B. Murray, in *The Physics of Ultra-High-Density Magnetic Recording*, edited by M. L. Plumer, J. v. Ek, and D. Weller (Springer, New York, 2001), pp. 249–276.
- ¹⁹L. Menon, M. Zheng, H. Zeng, S. Bandyopadhyay, and D. J. Sellmyer, *J. Electron. Mater.* **29**, 510 (2000).
- ²⁰D. Navas, M. Hernández-Vélez, M. Vázquez, W. Lee, and K. Nielsch, *Appl. Phys. Lett.* **90**, 192501 (2007).
- ²¹S. Taketomi, *Jpn. J. Appl. Phys., Part 1* **22**, 1137 (1983).
- ²²S. Pu, X. Chen, Y. Chen, Y. Xu, W. Liao, L. Chen, and Y. Xia, *J. Appl. Phys.* **99**, 093516 (2006).
- ²³H. -E. Horng, S. Y. Yang, S. L. Lee, C. Y. Hong, and H. C. Yang, *Appl. Phys. Lett.* **79**, 350 (2001).
- ²⁴W. Luo, T. Du, and J. Huang, *Phys. Rev. Lett.* **82**, 4134 (1999).
- ²⁵A. Bourlino, A. Simopoulos, D. Petridis, H. Okumura, and G. Hadjipanayis, *Adv. Mater.* **13**, 289 (2001).
- ²⁶S. Ohya, K. Ohno, and M. Tanak, *Appl. Phys. Lett.* **90**, 112503 (2007).
- ²⁷J. L. Mene'ndez, B. Besco's, G. Armelles, R. Serna, J. Gonzalo, R. Doole, A. K. Petford-Long, and M. I. Alonso, *Phys. Rev. B* **65**, 205413 (2002).
- ²⁸B. R. Jennings, M. Xu, and P. J. Ridler, *Proc. R. Soc. London, Ser. A* **456**, 891 (2000).
- ²⁹M. Tadic, V. Kusigerski, D. Markovic, I. Milosevic, and V. Spasojevic, *Mater. Lett.* **63**, 1054 (2009).
- ³⁰E. Fonda, S. R. Teixeira, J. Geshev, D. Babonneau, F. Pailloux, and A. Traverse, *Phys. Rev. B* **71**, 184411 (2005).
- ³¹E. E. Shalyguina, I. Skorvanek, P. Svec, V. A. Melnikov, and N. M. Abrosimova, *J. Exp. Theor. Phys.* **99**, 544 (2004).
- ³²Y. Yao, H. C. Mireles, J. Liu, Q. Niu, and J. L. Erskine, *Phys. Rev. B* **67**, 174409 (2003).
- ³³M. Tadic, V. Kusigerski, D. Markovic, I. Milosevic, and V. Spasojevic, *J. Magn. Magn. Mater.* **321**, 12 (2009).
- ³⁴B. Dieny and J. P. Gavigan, *J. Phys.: Condens. Matter* **2**, 187 (1990).
- ³⁵A. Imre, G. Csaba, L. Ji, A. Orlov, G. H. Bernstein, and W. Porod, *Science* **311**, 205 (2006).